Processing and Characterization of Thermally Cross-Linkable Poly[*p*-phenyleneterephthalamide-*co*-*p*-1,2-dihydrocyclobutaphenyleneterephthalamide] (PPTA-*co*-XTA) Copolymer Fibers

Tao Jiang, Jennifer Rigney, Marie-Christine G. Jones, Larry J. Markoski, Gary E. Spilman, Deborah F. Mielewski, and David C. Martin*

Department of Materials Science and Engineering and the Macromolecular Science and Engineering Center, The University of Michigan, Ann Arbor, Michigan 48109-2136

Received November 21, 1994; Revised Manuscript Received February 15, 1995®

ABSTRACT: A scheme was developed to cross-link poly(*p*-phenyleneterephthalamide) (PPTA or Kevlar) in order to modify its macroscopic properties. The method is based on incorporating XTA, a benzocyclobutene-modified derivative of terephthalic acid, into the polymer backbone and then inducing cross-linking by heat treatment after the fiber is formed. PPTA-*co*-XTA copolymers with various XTA contents exhibited lyotropic nematic liquid crystalline behavior and could be spun into fibers by dry-jet wet spinning techniques. As-spun fibers were heat-treated at intermediate temperatures (200–300 °C) to increase crystallinity and orientation and at higher temperatures (above 320 °C) to trigger cross-linking. Wide angle X-ray diffraction confirmed high molecular orientation in the fibers before and after cross-linking. The mechanical properties of these fibers were studied as a function of XTA content and conditions of heat treatment. Cross-linked copolymer fibers generally showed an improvement in tensile modulus over as-spun fibers. For the PPXTA homopolymer, however, the tensile strength and toughness tended to decrease with increasing length and temperature of the heat treatment. FTIR and ESR spectroscopic studies suggested this resulted from a degradative chain scission process. Compressive properties of these fibers were investigated through elastica and recoil tests, and through measurement of the fiber critical strain to kinking in a beam bending geometry. The strain to induce kinking in cross-linked PPXTA fibers is approximately twice that of the un-cross-linked material. The copolymer fibers also exhibited increased resistance to creep and lateral deformation after heat treatment.

Introduction

As a high-performance extended-chain polymer, poly(*p*-phenyleneterephthalamide) (PPTA or Kevlar) has received considerable attention since it was reported by Kwolek in 1972.[1] The commercial and scientific interest

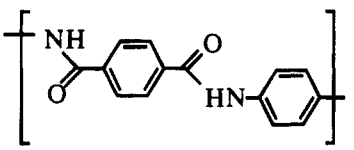

PPTA

of this and similar materials such as poly(*p*-phenylenebenzobis(thiazole)) (PBZT) and poly(*p*-phenylenebenzobis(oxazole)) (PBZO) arises from their high tensile moduli and strengths in fiber form (modulus ca. 100–350 GPa, tensile strength ca. 2.0–3.5 GPa). These properties can be attributed to structural characteristics including stiff, extended-chain conformation and high molecular orientation. A major drawback of these materials, however, is the relatively low compressive strengths (about one-tenth of the tensile strengths).[2,3] This imbalance in mechanical properties severely limits their potential in structural applications. The compressive weakness is generally believed to arise from the kinking or buckling of the polymer chains due to a lack of strong lateral intermolecular bonding.[4,5] Hence the introduction of covalent cross-links between the macromolecular chains is expected to help overcome these poor compressive properties. This leads to the concept of a three-dimensional ordered polymer network with intermediate structural characteristics between carbon fibers (strong in tension and compression, yet brittle) and normal extended-chain polymer fibers (strong in tension, tough, yet weak in compression) (Figure 1) (adapted from ref 18). By controlling the amount and distribution of cross-linking, it should be possible to tune the mechanical properties between these two extremes.

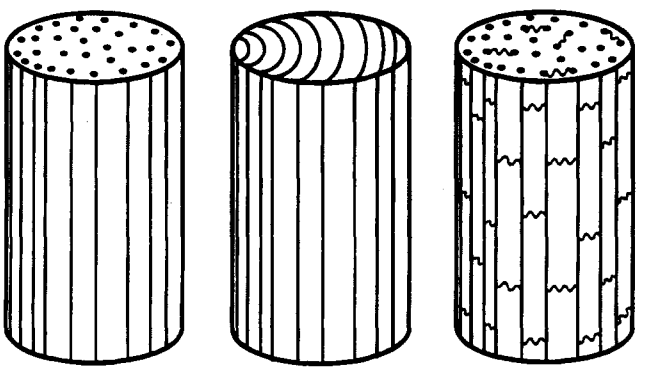

Figure 1. Structural characteristics of (a) extended-chain fiber, (b) carbon fiber, and (c) cross-linked extended-chain fiber.

Other properties of aramid fibers could also be altered by intermolecular covalent bonding. Studies have shown the relationship between the moisture-dependent creep behavior and the crystallite slip or rotation in PPTA fibers.[6] Covalent cross-links between crystallites might limit this structural maneuverability and therefore reduce creep. Cross-linking is also expected to help improve fiber abrasion resistance and fiber–matrix adhesion. In addition, thermally activated cross-linking agents might provide a mechanism for higher flame resistance.

There have been several attempts to enhance lateral interactions in aromatic polymer fibers.[7,8] Significant

* To whom correspondence should be addressed.
® Abstract published in *Advance ACS Abstracts,* April 1, 1995.

0024-9297/95/2228-3301$09.00/0 © 1995 American Chemical Society

improvements in compressive performance, however, have not yet been demonstrated. Sweeny reported a cross-linking method based on thermolysis of active aryl halides in the polymer unit and coupling via free radicals.[9] The approach worked well for PBZT and improvements in fiber compressive strength and shear modulus were achieved. Unfortunately, the improvement came at the cost of decreased tensile properties, resulting possibly from the loss of mass upon reaction and the disappearance of lyotropic liquid crystalline behavior at high densities of the cross-linking agent.

It is possible to achieve lateral covalent bonding in polymers by incorporating into the molecular backbone a thermally activated cross-linking agent 1,2-dihydrocyclobutabenzene-3,6-dicarboxylic acid (XTA). This

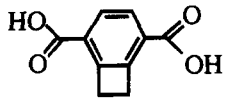

XTA

monomer contains the benzocyclobutene (BCB) moiety which is a thermally reactive cross-linkable group.[10] The principles of this approach were based on the hypothesis that the BCB groups should lie dormant during synthesis and fiber formation and could then be triggered into reactive states via heat treatment at temperatures well below degradation with no mass loss. These properties together with the high molecular aspect ratio necessary to preserve the liquid crystalline behavior make it possible to produce cross-linked yet highly oriented fibers.

A similar approach was recently reported by Rickert *et al.*[11,12] They synthesized 2,2,6,6-tetraoxo-1,3,5,7-tetrahydro-2,6-dithia-*s*-indacene-4,8-diimine (DSDA), a derivative of *p*-phenylenediamine. DSDA contains two five-membered rings which undergo a thermally induced ring-opening reaction with the release of SO_2. DSDA was copolymerized with *p*-phenylenediamine and terephthaloyl dichloride. Only those copolymers with lower than 20 mol % DSDA in the total amount of diamines were soluble in sulfuric acid and could be spun into fiber. The molecular orientation of the fiber was poorer compared to that of PPTA. No improvement of the compressive strength for the cross-linked fiber was found, and the overall mechanical properties apparently deteriorated with increasing DSDA content. The possible causes for these observations include (1) the bulkiness of the DSDA structure, (2) the mass loss during heat treatment due to SO_2 release and (3) the competition between cross-linking and structural reorganization due to the low cross-linking temperatures. All of these limitations should be circumvented in the XTA copolymer system.

High-performance aromatic polymer fibers including PPTA are usually produced by dry-jet wet spinning techniques. Due to the inherent similarities between PPTA and the PPTA-*co*-XTA copolymers we made by

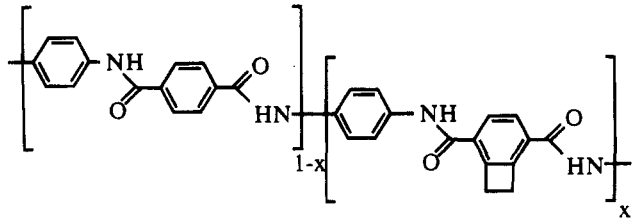

PPTA-co-XTA

incorporation of the XTA, we anticipated that the basic principles of the dry-jet wet spinning procedures could also be employed in the processing of the new copolymer fibers. Because of the unique reactivity of the XTA unit, however, more efforts needed to be made especially on the spinning solution preparation and characterization, and more sophisticated postspun heat treatment schemes needed to be designed. Furthermore, it was expected that the new copolymer fibers would process molecular orientation and crystalline structures similar to those of the neat PPTA fiber which are well understood.[13-16]

PPTA-*co*-XTA copolymers with various mole percentages of XTA were synthesized by condensation polymerization of terephthaloyl chloride, the diacid chloride of XTA, and *p*-phenylenediamine.[17-19] Here we describe the processing of PPTA-*co*-XTA fibers through dry-jet wet spinning techniques and the characterization of their macroscopic properties.

Experimental Procedures

Processing. Like many high-performance aramid fibers, the PPTA-*co*-XTA copolymer fibers were produced from solution. In preparing the spinning dope, the PPTA-*co*-XTA copolymer with inherent viscosity ranging from 4.5 to 5.5 dL/g was first mixed in a beaker with concentrated sulfuric acid (100% H_2SO_4) by mechanical stirring. The polymer concentration of the solution was 18% (by weight). The mixture was then transferred into a mixing device consisting of two interconnected cylinders. The mixture was pushed from one cylinder to the other through a screen pack by compressed gas until a homogeneous solution was formed. The cylinder was surrounded by a band heater and the mixing was carried out at about 80 °C. Prolonged exposure to higher temperatures was avoided to prevent degradation or cross-linking of the copolymers. The dopes thus prepared were examined in a cross-polarized optical microscope equipped with a Mettler FP800 hot stage to check the homogeneity and liquid crystalline behavior.

The dry-jet wet spinning method developed by Blades[20,21] is generally employed in the processing of high-performance aromatic polymer fibers. During the process, the out-flowing jets of polymer solution pass through an air gap before entering the coagulation bath.

The spinning of cross-linkable PPTA-*co*-XTA copolymer fibers was carried out on a small scale extrusion apparatus obtained from Bradford University Research Ltd. It consisted of four components: (1) extrusion system, a motor-driven screw jack, (2) spinning block, including a cylinder, a piston, a spinnerette, and a screen pack, all made of stainless steel, (3) coagulation bath, and (4) take-up unit. About 5 mL of polymer solution was loaded into the extrusion cylinder and extruded through the spinnerette orifice. The diameter of the orifice varied from 80 to 250 μm, with the same aspect ratio (L/D) of 1. Filament velocities at the orifice ranged from 10 to 50 m/min, depending upon the advancing speed of the piston and the diameter of the orifice. The processing temperatures were selected through the thermal analysis and the optical microscopic study of the dopes. Typically, the spinning temperatures were around 60–70 °C. The filament passed initially through an air gap of 10–20 mm and then through the coagulation bath (water or dilute acid solution) at room temperature along a path of 80 cm in length. The coagulated filament was finally collected on a spool by the take-up unit. The take-up velocities varied from 30 to 110 m/min, resulting in spin stretch factors of 2–5. The collected fibers were neutralized overnight in 0.5 wt % NaOH solution, washed thoroughly in water (70 °C) and dried in air.

In the processing of conventional high-performance aromatic fibers, the thermal treatment of as-spun fibers promotes orientation and crystallinity and therefore enhances the tensile properties.[22-24] For our PPTA-*co*-XTA fibers, subsequent heat treatment is of particular importance since both physical and chemical changes may occur during the process.

The apparatus for the heat treatment of PPTA-*co*-XTA fibers consisted of a laboratory-size furnace with automatic temper-

ature control, a fiber supply spool and a take-up spool (Bradford University Reseach Ltd.). The furnace was flushed with nitrogen throughout the process. The residence time was about 10 s. A small amount of tension was applied by maintaining a slight difference between the speeds of the two spools. The resulting stretch was about 10% in most cases.

The characteristic temperatures required for heat treatment were determined by thermal analysis. Differential scanning calorimetry (DSC) studies of the PPTA-*co*-XTA copolymers showed that the solid-state cross-linking reactions occurred within the range 325–425 °C, with the maximum of the reaction exotherm located at about 380 °C.[17–19] Thermogravimetric analysis (TGA) confirmed that the copolymers exhibited no significant mass loss at those temperatures. To further understand the relationship between the state of cross-linking of the fibers and heat treatment conditions, systematic investigations were performed on the PPTA-*co*-100XTA fibers using a Perkin-Elmer 7 series thermal analysis system. Small amounts of fiber samples sealed in DSC pans were heated at a rate of 300 °C/min to a series of selected temperatures, held at those temperatures for 12 s, and rapidly cooled to room temperature. Then a second run was started at a heating rate of 15 °C/min until the samples decomposed. In the first run a fiber sample with a certain degree of cross-linking was obtained while in the second run the exothermal reaction heat for that sample was acquired. By comparison with that of the as-spun fiber as a control, we were able to determine the relative degree of reaction corresponding to the particular heat treatment temperature.

Structural Evaluation. Wide angle X-ray diffraction (WAXD) data were collected on PPTA-*co*-XTA copolymer powders. We used a Rigaku Rotaflex diffractometer operated at 40 kV and 100 mA with a Cu target (0.154 nm) and graphite monochromator. The scanning speed was selected to be 2°/min with a 0.01° increment.

WAXD fiber patterns were obtained from bundles of parallel fibers mounted perpendicular to the X-ray beam on a Statton camera. The radiation was generated by a Philips X-ray unit with an Fe target (0.194 nm) and a Mn filter. Diffraction patterns were recorded on Kodak Diagnostic X-ray films. Ni single crystal powders were used as a standard to calibrate the camera length.

The presence and degree of cross-linking in the heat-treated fibers were examined by swelling experiments. A small piece of fiber (200–400 μm in length) was placed on a glass slide with a few drops of sulfuric acid (96%) nearby. The slide was then put into a glass chamber flushed with dry nitrogen and sealed to prevent the absorption of water by the acid. The chamber was placed on the stage of an optical microscope and tilted so that the acid came into contact with the fiber. The behavior of the fiber in the acid was then videotaped and measured.

Fourier transform infrared spectroscopy (FTIR) was obtained on a Mattson Galaxy Series FTIR-3000 system in order to study the mechanisms of the cross-linking reaction and possible thermal degradation. Data were collected on PPTA-*co*-XTA copolymer powders heat-treated under different temperatures. Samples were mixed with KBr single crystal powders, and the diffuse reflection mode was used.

Mechanical Tests. Tensile tests were carried out on an Instron 4204 testing frame equipped with an Omega 1000 g capacity load cell and fiber grips. A cross-head speed of 1 mm/min and a gauge length of 1 in. were used. The load–displacement curves were recorded on a strip chart recorder. The fiber diameter was measured using an optical microscope attached to a Macintosh Quadra 700. The image-processing program NIH Image was then used to determine the widths of the fibers. The machine compliance was determined according to ASTM standard D3379.

The toughness of the fibers were measured by scanning the load–displacement curves into another imaging program, Adobe Photoshop. The digitized curves were "filled in" and opened in NIH Image where the number of pixels under the curve was measured and then translated into energy.

Fiber compressive strength was measured by means of the tensile recoil test.[2] Recoil forces acting on the broken ends of a fiber after tensile failure can cause substantial damage to high-performance fibers. This damage results from the compressive stresses developed during snap-back of the broken fiber which exceeds its compressive strength. By gradually increasing the tensile stress, a threshold stress for observation of the recoil damages is determined and used as a measure of fiber compressive strength. The test was done using the same equipment as in the tensile test. A pair of sharp surgical scissors mounted on a stand was used to ensure stable, symmetric cuttings.

Elastica tests were also used to obtain an estimate of the fiber compressive properties. The method was developed in 1950 by Sinclair to study the compressive behavior of glass fibers.[25] In the test the fiber was twisted to form a loop. As the fiber loop is drawn down, the ratio of the major and minor axes should remain constant at about 1.34 until the fiber is damaged, either by kinking (on the interior) or tensile failure (on the exterior). For anisotropic fibers compressive failure typically occurs before tensile failure. The strain at either surface of the fiber may be calculated from the major axis of the loop (M) and the radius of the fiber (R):

$$\epsilon = \pm R/0.350M$$

The critical strain where the ratio of the axes deviates from its original value gives an estimate of the compressive strain to failure.

In our tests, the fiber was taped at one end to a glass slide and twisted at the other end to form a loop. A drop of microscope immersion oil was placed at the center of the loop and a glass coverslip placed on top, covering the loop but leaving the free end outside. The slide was placed under a Nikon SMZ-27 stereoscope attached to a Sony CCD camera. The free end of the fiber was slowly pulled to draw down the loop. The test was continued until the fiber broke or the loop was completely drawn down. The video was then imported into the NIH Image to measure the major and minor axes of the loop.

The compressive failure strains associated with the visualization of kink bands were measured with the beam-bending test.[26] In this test, the fiber was bonded to the surface of a polycarbonate beam. The beam was bent by inserting a block under one edge with the other edge fixed, and the fiber was subjected to the surface strain of the beam. By using an optically clear acrylic spray adhesive and a transparent polycarbonate beam, compressive failure or kinking could be observed with an optical microscope. The strain ϵ required to initiate failure was determined from the geometry of the bent beam and the distance x between the first kink observed and the fixed edge of the beam. The relationship is given by the following equation:

$$\epsilon(x) = \frac{3dt}{2L^2}\left(1 - \frac{x}{L}\right)$$

where d is the deflection of the beam, e.g. the high of the block, t is the thickness of the acrylic beam (1.9 mm), and L is the length of the beam between supports.

Creep tests were performed on fibers as well. Cardboard tabs were epoxied to the ends of long fibers (~15 cm). Reference marks were made on the fiber approximately 10 cm apart. The fibers were hung from a stand and preloaded with a paper clip (~0.4 g) before measurements of their initial lengths were made. Fibers were loaded to stresses of approximately one-third their tensile strength. Once the fiber was loaded, the distance between the marks was monitored as a function of time with a PTI traveling microscope which was used for accurate measurement in large length scale.

Experiments were carried out to study the lateral compressive behavior of fibers as a function of cross-link density. Sample fibers were mounted on a flat surface (glass microscope slide) and compressed laterally by a glass pipet (1 cm in diameter) with a series of dead loads (Figure 2). The deformed samples were examined in the optical microscope and SEM to determine the change in diameter and morphology upon deformation.

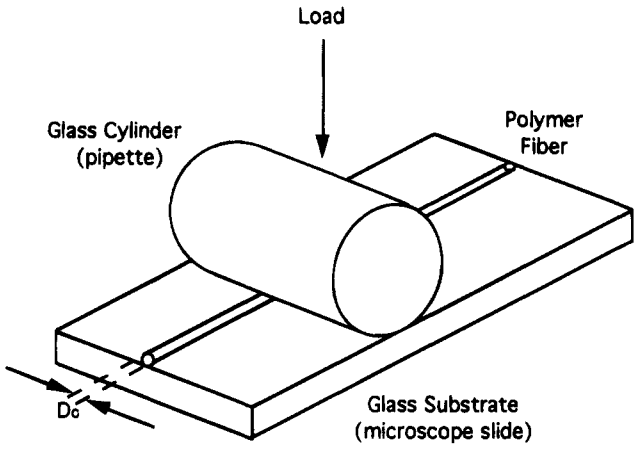

Figure 2. Schematic of the lateral compression test.

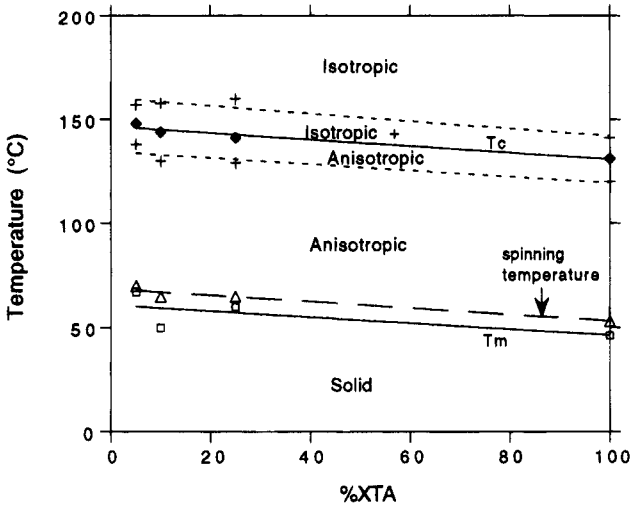

Figure 3. Phase transition temperatures of PPTA-*co*-XTA copolymer solutions (18 wt % in sulfuric acid).

Results and Discussion

Solution Characterization. The spinning dopes prepared from the PPTA-*co*-XTA copolymers were similar to those from normal PPTA. They were green-yellow solids at room temperature. With increased temperatures they softened and melted. When a thin layer of the dope was placed on a hot stage and examined in a cross-polarized optical microscope, an increase in intensity of the transmitted light was observed as the temperature reached a point, i.e., the apparent melting temperature (T_m).[20,21] Above this temperature the dope was optically anisotropic and exhibited birefringent textures, indicating the existence of nematic liquid crystalline phases. The melting temperature apparently represents a transition from a solid crystal solvate phase to the nematic liquid crystalline phase. When the temperature was raised further, a point was reached (T_c) at which the anisotropic phases began to disappear and the solution turned clear. A plot of T_m and T_c as a function of XTA percentage is shown in Figure 3. The transition temperatures decreased linearly with increasing XTA content. It was also noticed that there was a two-phase region around T_c where isotropic and anisotropic phases coexisted. The width of this region could be used as a measure of the dope quality.

The relationship between the clearing temperature T_c and the copolymer composition can be used to analyze the local environment in the solution in light of the Maier–Saupe theory[27] and its modification by Picken.[28] According to the theory, the nematic–isotropic transition temperature is proportional to the strength of a mean potential leading to the liquid crystal orientation. The observed decreasing transition temperatures imply weaker interactions between PPTA-*co*-XTA molecules in the solutions as the XTA content increases.

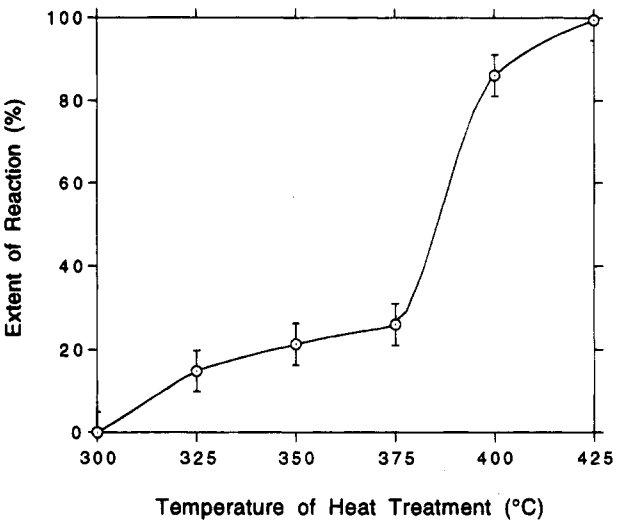

Figure 4. Extent of cross-linking reaction as a function of heat treatment temperature for the PPTA-*co*-100XTA fiber.

Fiber Spinning and Heat Treatment. In the phase transition diagram of the spinning dope (Figure 3), the spinning temperatures should lie in the anisotropic region in order to produce highly oriented fibers. In practice they were chosen to be slightly (about 10 deg) above T_m in an effort to minimize degradation.

The copolymer fibers we spun resembled commercial PPTA fiber (Kevlar) but were thicker (50–80 μm in diameter). When the residual acids were completely removed, the fibers were stable and remained yellow in air, otherwise they tended to turn brown with time. In the optical microscope, the fibers were less transparent than the commercial fibers, indicating higher defect densities. Defects were indeed seen by SEM both on the skin and in the core. These probably originated from trapping of disclination and domain wall defects present in the ordered nematic mesophase.[29]

The heat treatment temperatures for the as-spun fibers were determined through thermal studies. Figure 4 shows a plot of the extent of cross-linking reaction in PPTA-*co*-100XTA fibers calculated from the relative amount of exothermal heat detected in the DSC as a function of annealing temperature. The reaction apparently started at 300 °C and completed at about 425 °C. The extent of reaction increased with increasing annealing temperature with a sharp rise around 380 °C, which coincided with the exotherm maximum.

It is interesting to notice the association between the color of the heat-treated fiber and the annealing temperature. The polymers turned darker with increasing temperature, from light yellow before heat treatment to bright yellow at 350 °C, and to orange red around 400 °C when the cross-linking reaction was almost completed. It was also found that the higher XTA content the copolymer had, the darker the heat-treated fiber would be.

The DSC data suggested that temperatures higher than 425 °C were needed to fully induce cross-linking. Yet temperatures in that range could possibly cause more degradation of the polymers. In fact, thermogravimetric analysis (TGA) confirmed a weight loss of 1–3% in the copolymers at 450 °C.[19] Considering the fact that the maximum of the reaction exotherm was

Table 1. Exothermal Reaction Heat Data

sample	reacn heat (kcal/mol of BCB)	rel efficiency (%)
XTA diamide model compd	20.5	100
PPTA-*co*-100XTA fiber	15.7	77
PPTA-*co*-100XTA powder	10.2	50

around 380 °C, it appeared that temperatures between 380 and 400 °C were appropriate to trigger the cross-link reaction in the as-spun fibers.

It should be recognized that the completion of reaction of 425 °C in the copolymers does not necessarily mean that all the existing BCB groups have participated in cross-linking. Table 1 lists the exothermal reaction heat for XTA diamide model compound, PPTA-*co*-100XTA fiber and PPTA-*co*-100XTA powder. The data show that the cross-linking reaction in the model compound has the highest efficiency, apparently because these are small molecules and react in the liquid state and therefore have higher mobilities. The reaction efficiencies are lower for both PPTA-*co*-100XTA fiber and bulk polymer (77% and 50%, respectively, compared with that in the model compound). It is interesting to see that the fiber has a higher efficiency than the bulk polymer, perhaps because the organization of the macromolecules in the fiber results in clustering or a preferred orientation of the reactive moieties.

Swelling Experiments. The cross-linking of the copolymer fibers was examined by swelling experiments. The as-spun fibers and the fibers annealed below 300 °C were found to dissolve in concentrated sulfuric acid after about 15 min. In contrast the fibers heat-treated above 330 °C were insoluble. Instead, they swelled in the radial direction and shrank in the axial direction, leading to increased overall volumes. This swelling behavior confirmed the formation of a network of cross-linked molecules. Figure 5 shows a plot of the radial swelling ratio (D/D_o) as a function of annealing temperature for PPXTA fiber. Lower swelling ratios, an indication of higher cross-link densities, were associated with higher heat treatment temperatures.

The swollen fibers were observed in a cross-polarized optical microscope. After swelling, the copolymer fibers with low cross-link densities were optically isotropic, whereas the more heavily cross-linked materials remained birefringent. This behavior is generally consistent with that anticipated by recent theoretical treatments[30] and requires further investigation.

Wide Angle X-ray Diffraction. We summarize here some major results of our structural investigations. Details of the microstructural characterization of the PPTA-*co*-XTA copolymer fibers have been presented elsewhere.[31]

WAXD data of the PPTA-*co*-XTA copolymer powders showed systematic variations as the XTA content changed. With lower XTA contents (<10%) the diffraction pattern were similar to those of the PPTA homopolymer. As the XTA percentage increased, they became noticeably different. There was no significant difference between the data from cross-linked and heat-treated but un-cross-linked samples of the same composition.

The flat film WAXD patterns of the as-spun fibers showed typical meridional and equatorial reflections related to the uniaxial orientation of the fibers. When the fibers were annealed (heat-treated below cross-linking temperatures) however, the WAXD patterns exhibited much sharper reflections and more off-axis spots arrayed on layer lines, indicating an increase of the three-dimensional order of the macromolecules

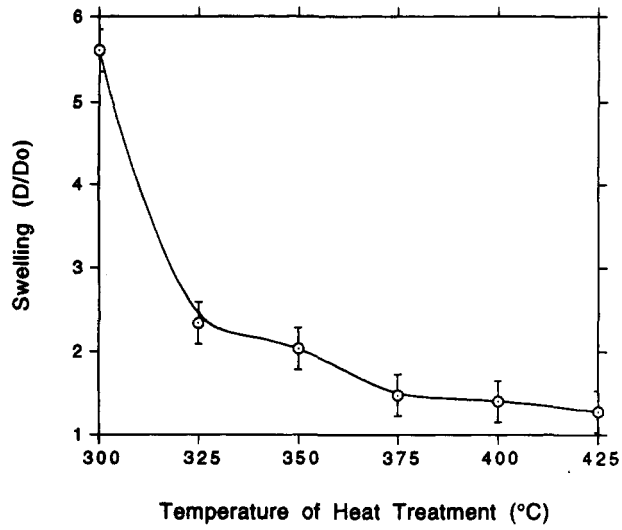

Figure 5. Radial swelling ratio of the PPTA-*co*-100XTA fiber in sulfuric acid as a function of heat treatment temperature.

Table 2. Orientation Angles of Heat-Treated Fibers

sample fiber	orientation angle (deg) (HT 260)	orientation angle (deg) (HT 400)
PPTA-*co*-5XTA		24
PPTA-*co*-10XTA	18	
PPTA-*co*-25XTA	16	18
PPTA-*co*-100XTA	12	14

(Figure 6a,b). Diffraction data of the cross-linked fibers were similar to those of the annealed but un-cross-linked fibers (Figure 6c), suggesting that the high orientation was retained after cross-linking. This indicates that the structural re-organization and the cross-linking reaction could be achieved at different temperature ranges.

The fiber X-ray patterns also gave information on the degree of molecular orientation in the fibers. Following procedures described by Alexander,[32] the arc lengths in degrees at the half-maximum density of the major equatorial diffraction peaks were measured and taken as the orientation angles of the samples. The results are presented in Table 2.

Tensile Properties. Various sample fibers were used in the tensile tests. In addition to the copolymer fibers processed at the University of Michigan, some of the copolymer powders were sent to DuPont for solution preparation and spinning. These include PPTA-*co*-5XTA and PPXTA. PPTA-*co*-5XTA as-spun and heat-treated (450 °C) fibers and PPXTA as-spun fibers were returned. The heat treatment of the DuPont-spun PPXTA fibers were done in batch mode since they were not continuously spooled. The heat treatment took place in a tube furnace with short pieces of fibers (~50 mm). A tension stage was built to apply a controlled amount of tension in the heat treatment.

Figures 7–9 show the tensile modulus, tensile strength, and fracture toughness data for the PPTA-*co*-XTA copolymer fibers spun in our laboratory as a function of the copolymer composition. In general, these properties improved slightly with increasing XTA content for both as-spun and heat-treated fibers, confirming that the substitution of XTA in PPTA does not cause a degradation in tensile properties. This is consistent with our findings that the substitution does not hinder the abilities of the molecules to exhibit lyotropic nematic mesophases and to form highly oriented and crystallized fibers. In contrast, Rickert et al. found that the best tensile properties of DSDA-substituted PPTA were at

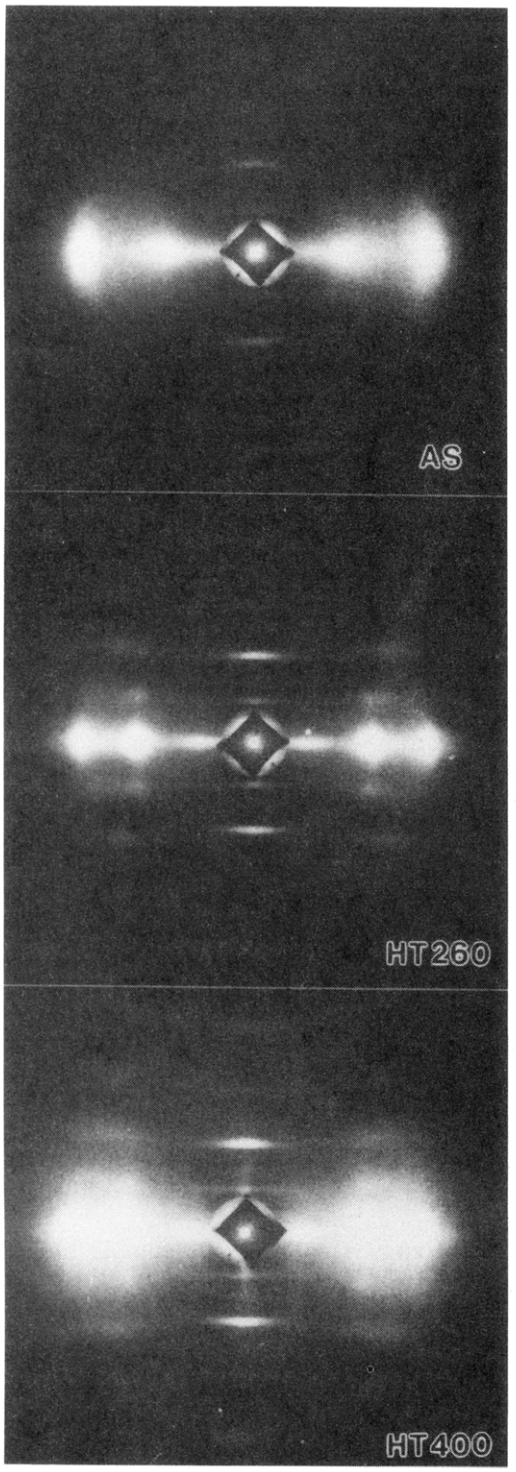

Figure 6. WAXD patterns of PPTA-*co*-100XTA copolymer fibers: (top) as-spun; (middle) heat-treated at 260 °C; (bottom) heat-treated at 400 °C.

low DSDA content and they decreased sharply with additional substitution,[11,12] probably due to a lower molecular aspect ratio and a loss of mass during cross-linking. At each composition, the tensile modulus of PPTA-*co*-XTA fibers had a tendency to increase with higher annealing temperature. The tensile strength was also found to improve upon cross-linking. However, the toughness dropped after heat treatment. This loss of toughness was most significant for cross-linked PPXTA fiber.

More detailed experiments were performed on the DuPont-spun PPXTA fibers due to its high XTA content and the amount of material available. The tensile modulus, strength, and toughness data are shown in Figures 10–12, respectively. Consistent with the earlier observations, the tensile modulus tended to increase with higher annealing temperature and longer heat treatment time. However the tensile strength of cross-linked PPXTA fibers experienced a dramatic decrease compared with those of the as-spun fibers. The fracture

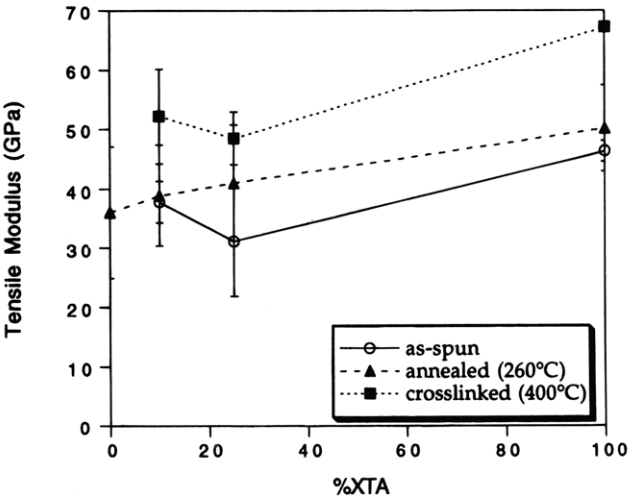

Figure 7. Tensile moduli of PPTA-*co*-XTA copolymer fibers spun at the University of Michigan.

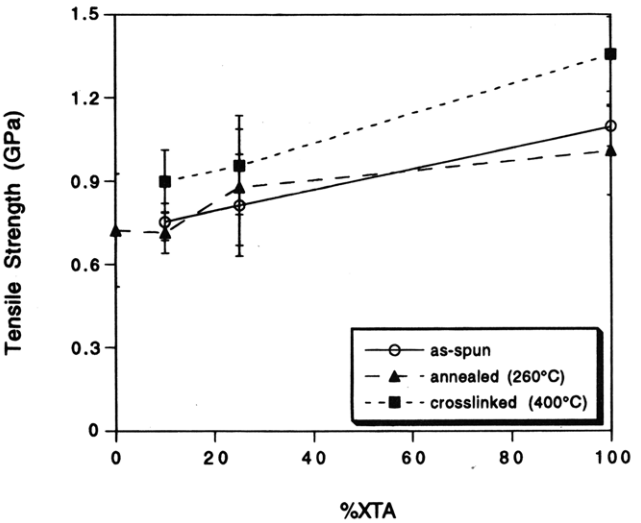

Figure 8. Tensile strengths of PPTA-*co*-XTA copolymer fibers spun at the University of Michigan.

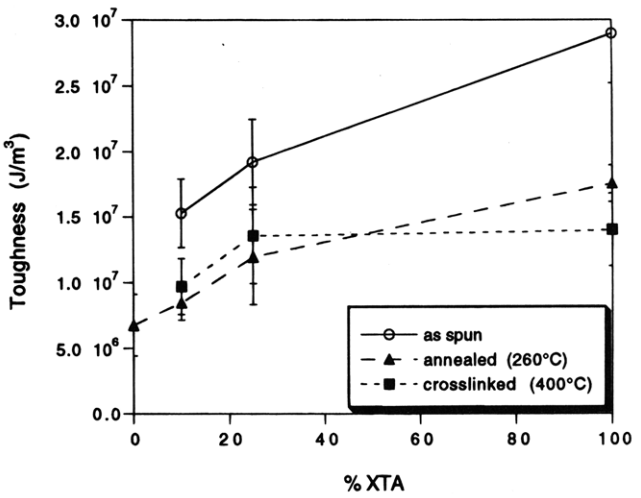

Figure 9. Toughness of PPTA-*co*-XTA copolymer fibers spun at the University of Michigan.

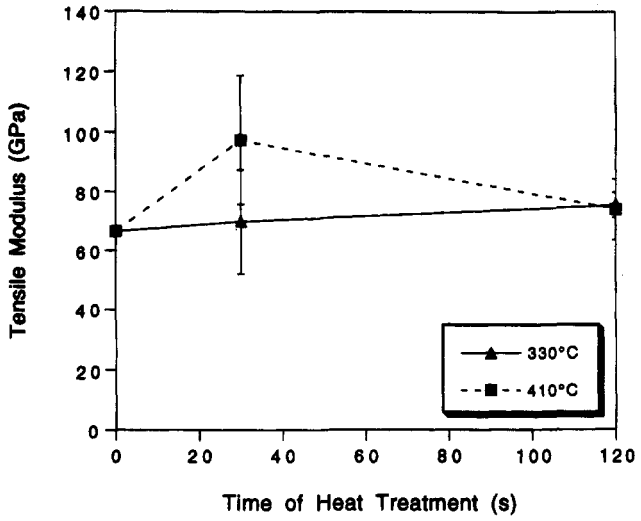

Figure 10. Tensile moduli of PPXTA fibers spun at DuPont.

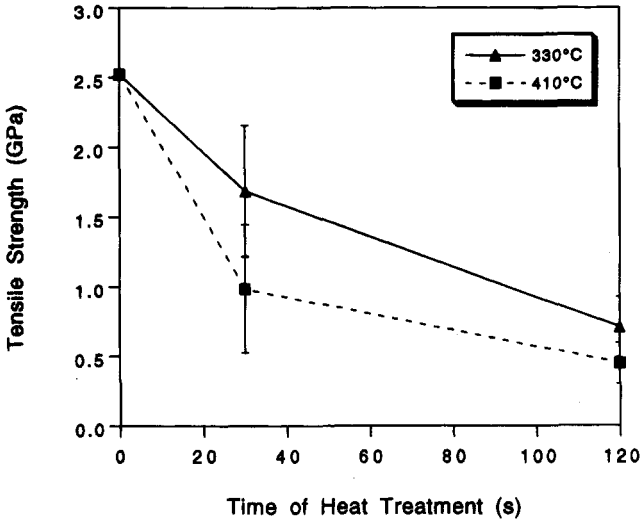

Figure 11. Tensile strengths of PPXTA fibers spun at DuPont.

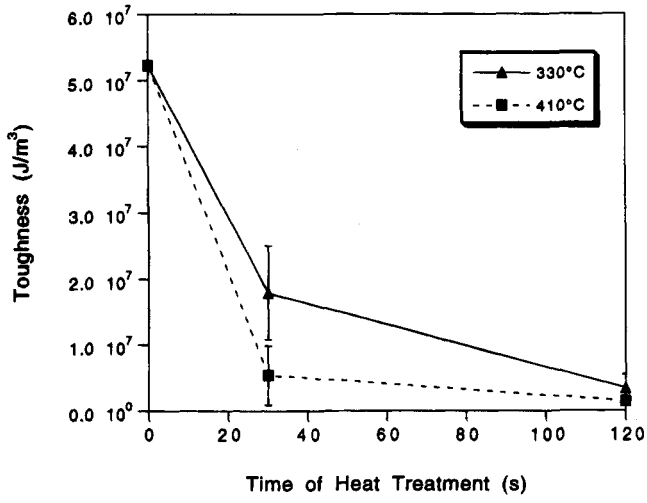

Figure 12. Toughness of PPXTA fibers spun at DuPont.

toughness also dropped correspondingly after heat treatment.

To understand the loss of tensile strength of cross-linked PPXTA fibers requires an analysis of the two classes of events concurring during heat treatment. One is a series of physical processes which involve structural re-organization leading to higher molecular orientation and crystallinity. The other is a series of thermally activated chemical reactions including cross-linking and possibly degradation. The physical processes typically increase both the tensile modulus and tensile strength of the heat-treated fibers, as demonstrated by similar behaviors of other high-performance fibers including PPTA. However, the chemical reactions, as implied by the experimental data, could result in a loss in tensile strength. The tensile properties of the heat-treated fibers are themselves the results of these competing processes. The experimental results suggest that the UM-spun and the DuPont-spun fibers are more sensitive to the physical and chemical processes, respectively. The diameters of DuPont-spun fibers are around 20 μm, whereas the UM-spun fibers have diameters ranging from 50 to 80 μm. Correspondingly, the latter consists of more structural imperfections, as mentioned before. The X-ray diffraction data showed that the UM-spun fibers exhibited higher misorientation angles and smaller crystallite sizes in the as-spun state compared to those of the DuPont-spun fibers. As a result, during the heat treatment the molecular orientation and crystallinity in the UM-spun fibers increased substantially, resulting in a much improved tensile modulus and strength even after compensation of the negative effect caused by the chemical reactions. For the DuPont-spun fibers, the molecular order and crystallinity in their as-spun state were already high, illustrated by the same tensile modulus (~67 GPa) as the cross-linked UM-spun PPXTA fiber, leaving little room for further improvement during annealing. Thus the effects of the chemical reactions dominated, leading to a loss in tensile strength. This phenomenon was most noticeable for the PPXTA homopolymer fiber because of its high XTA content.

The precise mechanisms for the loss of tensile strength due to the thermally activated chemical reactions remain to be fully explored. While the intended cross-linking reaction did occur in the heat treatment, other studies have suggested that the formation of cross-linking alone does not necessary result in reduced tensile strength. When working with cross-linkable high molecular weight polyethylene fibers, Penning et al. found that the cross-linked fibers have the same tensile strength and strain to failure as the un-cross-linked ones, although the cross-linking increased the interchain shear strength which led to a different, less fibrillar fracture surface.[33] We therefore presume that the loss of tensile strength is related to some thermal degradation concurrent with cross-linking during the heat treatment.

Degradation has been observed in other cross-linkable fiber systems. In his cross-linked polyamides, Sweeny saw a chain cleavage degradation through the rearrangement of the amide linkage to isocyanate.[9] Rickert et al. also found the generation of free radicals responsible for the poor mechanical properties in the heat-treated DSDA-containing copolymers.[11,12]

Electron spin resonance (ESR) spectroscopy performed on our PPXTA fibers heat-treated in the presence of oxygen showed the generation of free radicals. Moreover, the concentration of free radicals tended to increase with time, possibly leading to a propagation of degradative chain scission.[34]

Fourier transform infrared spectroscopy (FTIR) obtained from the heat-treated PPXTA polymers is shown in Figure 13. The disappearance of an absorption at 480 cm^{-1} for heat-treated samples (above 380 °C) is possibly associated with the activation of the BCB moieties as implied by infrared spectroscopy of other BCB-involving chemistry. As the annealing temperature increased, we saw the loss of a hydrogen-bonded

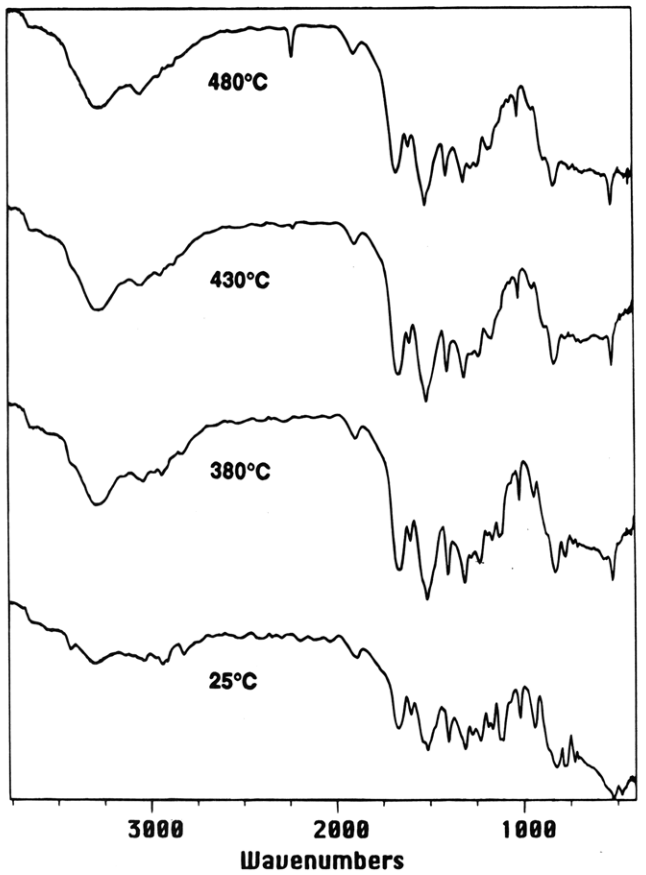

Figure 13. Infrared spectra of PPXTA powders heat-treated at various temperatures.

amide functionality (3432 cm^{-1}) and the appearance of isocyanate groups (2220 cm^{-1}), also an indication of thermal degradation.

Various schemes have been proposed for the BCB solid-state cross-linking reaction. Our spectroscopic studies have been consistent with the formation of a double-bonded carbon bridge between molecules, as also found by Marks et al. in BCB-modified polycarbonates.[35] Further work to identify the reaction intermediates and products will require more careful efforts with solid-state C^{13} NMR and FTIR or Raman studies on monomers with selected deuteration.

A close observation of the tensile fracture surfaces of the copolymer fibers revealed a morphological transition after heat treatment. The as-spun or mildly heat-treated fibers displayed a highly fibrillar fracture surface whereas the cross-linked fibers did not show such an extensive fibrillation (Figure 14). This morphological transition corresponds to a transition in failure mode from a slow, energy-absorbing fibrillar failure to a fast, brittle fracture. A similar transition was seen by Feldman et al. in a study of the tensile properties of poly(*p*-phenylenebenzobis(thiazole) (PBZT) films.[36] In this study, the morphology of samples after tensile failure exhibited a fibrillar–brittle transition when annealed at about 500 °C, accompanied by a decrease in tensile strength. Feldman et al. attributed this to thermal degradation. Sweeny also observed a change in tensile failure appearance of cross-linked PBZT fibers from fibrillar to brittle after a loss of 30% of the original halogen content and a decrease in tensile strength.[9] Taken together, these observations support the conjecture that the morphological transition and the decrease in tensile strength are both due to degradative chain scission.

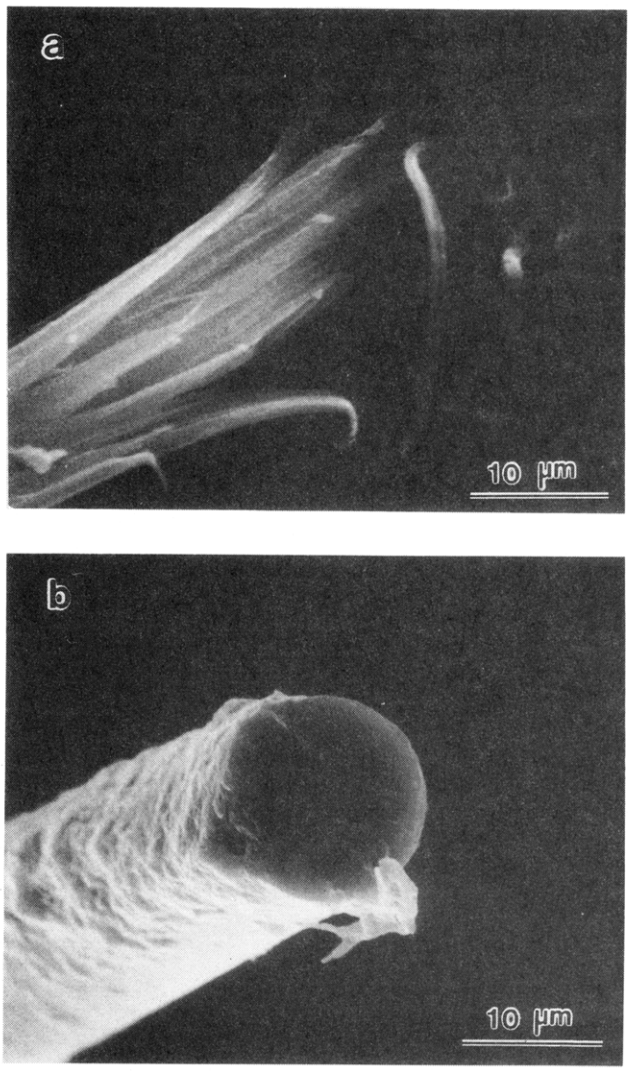

Figure 14. SEM micrographs of the tensile fracture surfaces of PPXTA fibers, showing a failure mode transition between fibers heat-treated at (a) 330 °C for 10 s and (b) 410 °C for 120 s.

To summarize, we present here a schematic diagram (Figure 15) to illustrate the molecular movements taking place inside the PPTA-*co*-XTA copolymer fibers during various steps of the processing scheme. During solution spinning, the phase separation upon coagulation resulted in a network of interconnected microfibrils in the as-spun fibers. When the as-spun fibers were heat-treated at a lower temperature, such as 250 °C, the molecules reorganized themselves and formed crystallized regions. However, the average size of the crystallites was small, resulting in a significant portion of the BCB moieties located in the less ordered grain boundary areas.[31] When the fibers were subjected to higher temperatures around 400 °C, the BCB moieties were triggered into reactive states and cross-links formed. Again, the cross-linking occurred mainly in the less ordered regions.[31] When the fibers were heat-treated at even higher temperatures, chain degradation dominated, leading to poor tensile strength.

Compressive Properties. For the tensile recoil tests, we were able to obtain reproducible results only on PPTA-*co*-5XTA fibers. For this low cross-link density material we observed a slight (14%) improvement of the compressive strength over the as-spun fiber (253 MPa for as-spun fiber and 288 MPa for cross-linked fiber).

In the elastica test, no well-defined critical strains could be identified for the PPTA-*co*-XTA samples. Thus

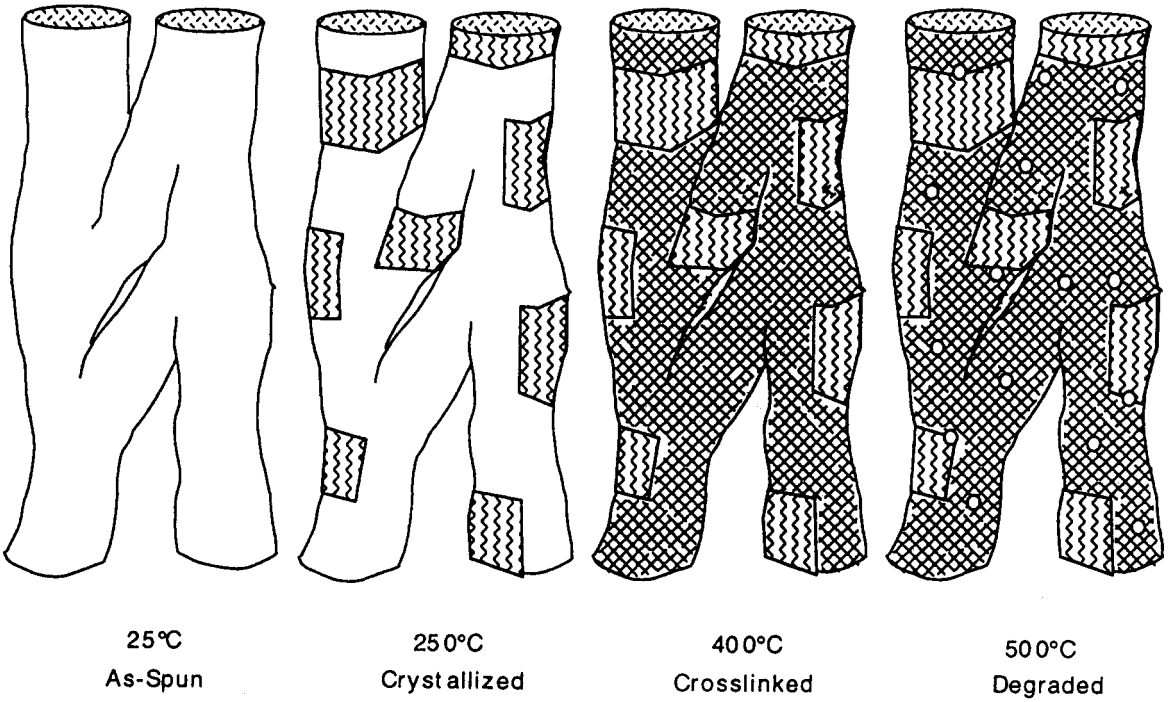

Figure 15. Schematic diagram illustrating the molecular movements in the copolymer fibers during processing.

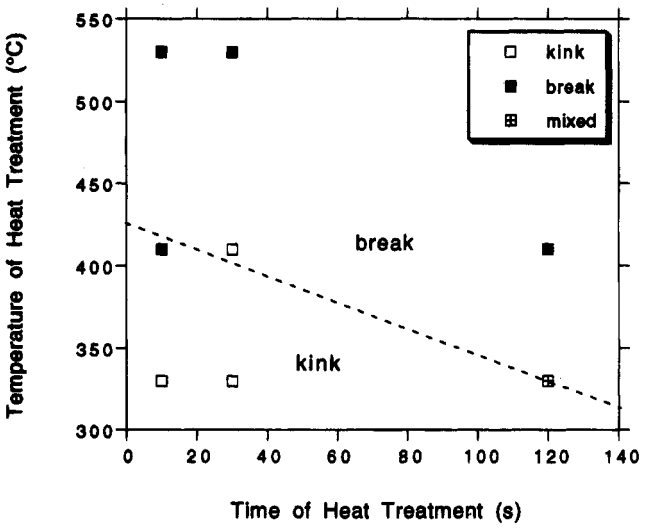

Figure 16. Transition of bending failure mode as a function of heat treatment conditions observed in the elastica test for PPXTA fibers.

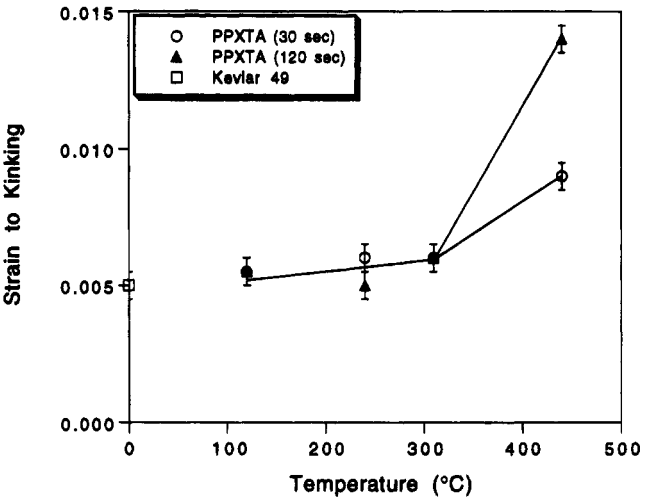

Figure 17. Critical strains to kinking for PPXTA fibers as a function of heat treatment conditions determined in the beam-bending test.

we were unable to use this test to estimate compressive properties. However, it was possible to see a transition of failure mode in the looped fibers from kinking to brittle fracture with increasing degree of heat treatment, corresponding to the morphological transition of fracture surfaces observed in the tensile test. Figure 16 shows the different failure modes of the copolymer fibers occurring in the elastica test as a function of heat treatment. This transition in failure mode is indicative of the competition between the increasing compressive strength and the decreasing tensile strength of the cross-linked fibers.

The critical strains to kinking of PPXTA fibers obtained in the beam-bending test are plotted as a function of heat treatment time and temperature in Figure 17. It was noticed that kinking persisted regardless of heat treatment conditions, even in the fully cross-linked PPXTA fiber.

The data in Figure 17 showed that the strains to kinking of heat-treated PPXTA fibers remained unchanged with increasing annealing temperature up to about 310 °C. After that the failure strains increased with higher temperatures. At 440 °C when the cross-linking reaction was completed, the strains to kinking were approximately 2–3 times of the original values depending on the length of the heat treatment. As discussed before, in the temperature range of about 100–300 °C, the cross-linking was not yet activated and the copolymer fibers underwent structural re-organization leading to higher orientation and crystallinity. The fact that the compressive strain to kinking remained constant during this period indicates that the improvement in molecular order does not affect the fiber compressive properties in terms of failure strain.

Creep and Lateral Deformation. The heat-treated PPTA-*co*-XTA fibers exhibited increased resistance to creep when compared to the as-spun fibers. Figures 18 and 19 show the observed creep and creep rate, respectively, for PPXTA fibers subjected to the same levels of stress and various heat treatment conditions. The amount of creep and the creep rate were found to

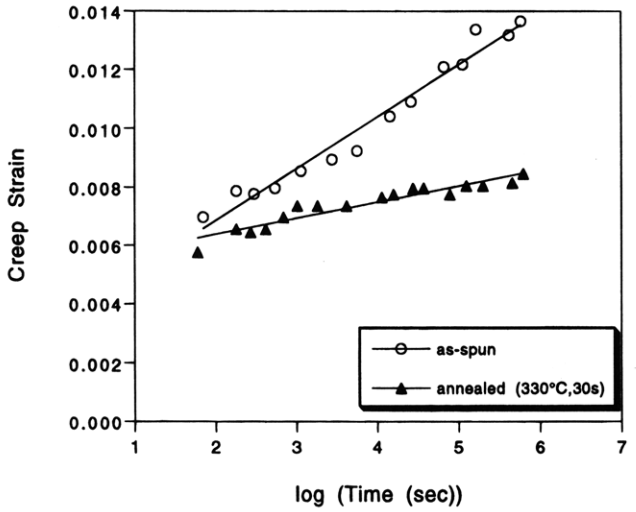

Figure 18. Creep strain of as-spun and heat-treated PPXTA fibers (σ = 390 MPa).

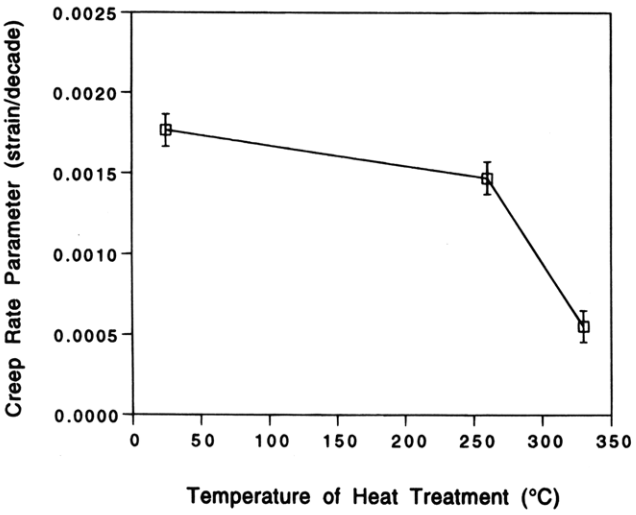

Figure 19. Creep rate parameters of PPXTA fibers (σ = 390 MPa) as a function of heat treatment temperature.

decrease with annealing (HT 260 °C) and drop sharply upon cross-linking (HT 330 °C).

Several theories have been proposed to explain the creep mechanisms for oriented high-modulus polymers such as PPTA. Wang et al. studied the moisture-dependent creep behavior in PPTA fibers.[6] One mechanism the authors suggested was that moisture interfered with hydrogen bonding in the structure and therefore caused accelerated crystallite slip or rotation. Ericksen also attributed creep of aramid fibers to crystallite rotation which resulted from the arrangement of intercrystallite bonds in the crystallite boundaries due to stress and thermal activation.[37] This crystallite movement is believed to be suppressed by covalent cross-linking which occurs preferentially in the grain boundary phase between crystallites, leading to reduced creep. Another theory proposed by Schuppert involved the transport of conformation defects of the molecules.[38] Again, this is expected to be restrained by the existence of intermolecular cross-links. Considering the fact that various processes occurred in the heat treatment, however, the exact mechanisms of this enhanced creep resistance need further study in order to separate the relative effects of cross-linking and molecular ordering.

Lateral compression tests were performed on the cross-linkable copolymer fibers, since we anticipated

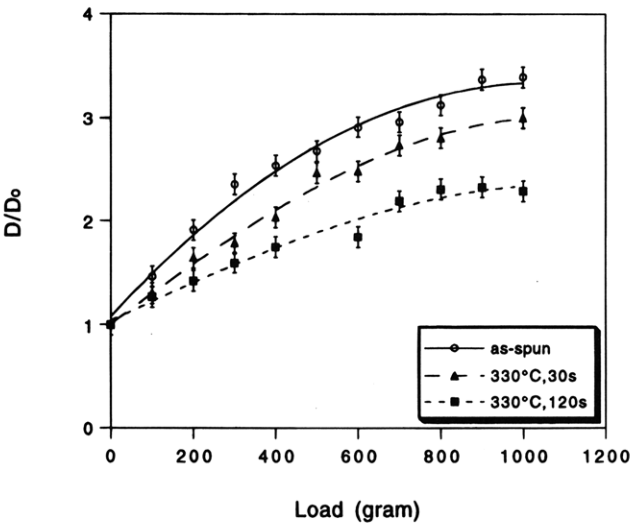

Figure 20. Diameter change of the laterally compressed PPXTA fibers subjected to various heat treatment conditions.

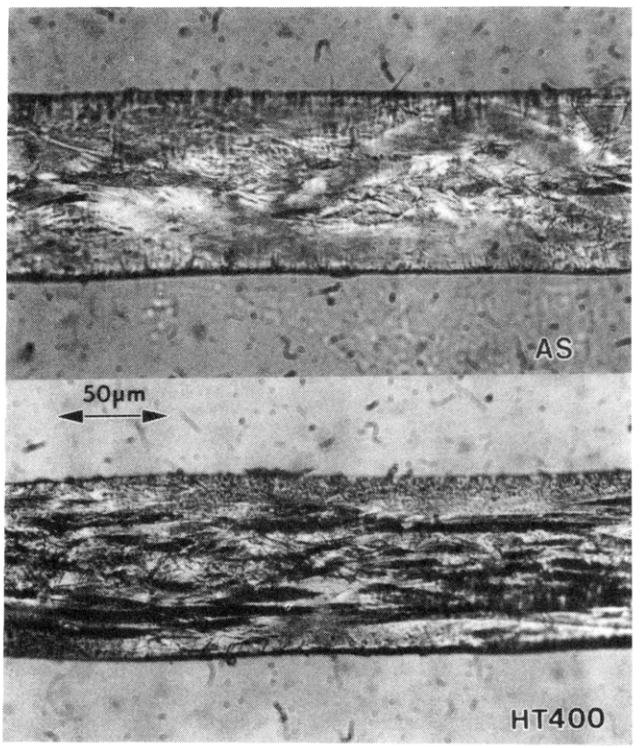

Figure 21. Optical micrographs of the deformed areas for the laterally compressed PPXTA fibers showing different morphologies between as-spun and cross-linked samples.

that the response of anisotropic fibers to lateral deformation would reflect the interactions between the molecules which should be altered by cross-linking. Figure 20 shows the diameter changes for laterally deformed PPXTA fibers heat-treated at 330 °C for various lengths of time. The fibers deformed less when they had been heat-treated for longer times, and therefore possessed higher cross-link densities. We believe that the interchain cross-links would increase the molecular interactions and restrain the relative shearing between molecules and crystallites which was likely to take place during lateral deformation, thus enhancing the fiber resistance to lateral compression.

When the laterally deformed fibers were examined in the optical microscope and the SEM, we observed strikingly different morphologies between the cross-linked and un-cross-linked fibers (Figure 21). The deformed areas of the un-cross-linked samples were flat

and smooth whereas the compressed cross-linked fibers exhibited cracklike textures parallel to the orientation direction. This is believed to be the consequence of the microfibrillar structure within the fibers. The microfibrillar boundaries in un-cross-linked fibers offered little resistance to external compression and the fibers deformed uniformly. When the fibers were cross-linked, however, the boundaries confined the cross-linking within the individual fibrils and created structural heterogeneities. These microfibril boundaries tended to fall apart under lateral compression and resulted in a different deformation morphology.

Future Development. As discussed above, the fact that kinking persists in the cross-linked PPXTA fiber suggests that the current XTA-substituted PPTA copolymer system has not yet been able to provide sufficient cross-link density in order to suppress kinking as the dominant compressive failure mode. Therefore we are developing a new series of XTA-related monomers which will incorporate more cross-linking functionality into the polymer backbone.[39]

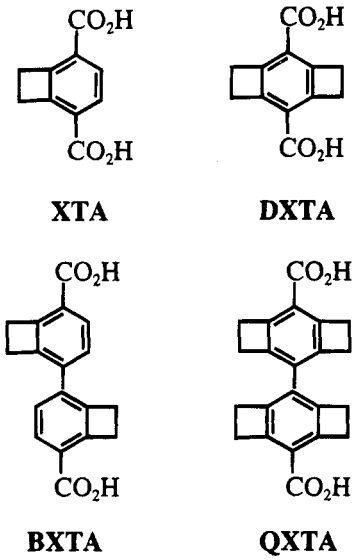

Furthermore, this new approach might also make it possible to introduce truly three-dimensional cross-linking into the structure because of different orientation of neighboring phenylene moieties.

It has been recognized that the compressive failure by kinking in extended-chain polymer fibers can initiate on the microfibrillar substructures developed during solution processing as well as on individual molecular chains.[40] In order to improve the compressive properties, it is evidently necessary to increase the lateral interaction both between the polymer chains and between the microfibrils. The lateral deformation experiment suggested that cross-linking in the PPTA-co-XTA fibers occurred only within, but not across, the microfibrillar boundaries. To address this problem, we are developing several new postspinning processing schemes:

(1) Multiple stage heat treatment. An initial treatment at lower temperatures is taken to increase the crystalline size and molecular orientation and to help eliminate microfibrillar boundaries. A second heat treatment is then followed to trigger the cross-linking reaction.

(2) High-pressure heat treatment. High isostatic pressure might squeeze the fiber and force the microfibrils close enough for the cross-linking reaction to take place.

(3) Fiber infiltration. Cross-linkable monomers can be infiltrated into the pore space between microfibrils to act as a bonding agent.

At the same time we are also working on cross-linkable thermotropic liquid crystal polymers including XTA-equipped aromatic polyesters (such as HBA/HNA) in order to circumvent the microfibril-related problems. However, microfibrils have also been found in these materials.[41,42] Therefore a successful scheme must involve a means to suppress the density fluctuations developed during precipitation from solution or cooling from the melt.

The degradative chain scission observed in the cross-linked PPTA-co-XTA fibers is another major concern that should be addressed in virtually any material with BCB chemistry. We are looking into possibilities of incorporating reactive agents into the fibers to saturate the double bonds and prevent the propagation of free radicals. Postprocessing halogenation is also currently under investigation.

Conclusions

High-concentration PPTA-co-XTA copolymer solutions (18 wt % in 100% sulfuric acid) possess lyotropic nematic liquid crystalline phases. The nematic–isotropic phase transition temperature decreases slightly with increasing XTA content.

PPTA-co-XTA copolymer fibers can be spun from sulfuric acid solution using dry-jet wet spinning techniques at temperatures well below the cross-linking temperature. The fibers maintain high molecular orientation and crystallinity.

As-spun fibers can be heat-treated at intermediate temperatures to improve the crystallinity and orientation, or at elevated temperatures to induce cross-linking with no mass loss.

DSC and swelling studies have confirmed the existence of cross-linking in heat-treated fibers. WAXD data show that high molecular orientation remains in cross-linked fibers.

The substitution of XTA in PPTA has been shown to occur without a degradation of tensile strength, modulus, and creep resistance, in both the as-spun and annealed states.

In XTA-rich PPXTA fibers, a decrease in tensile strength after cross-linking is observed. This is believed to result from a degradative chain scission reaction during the heat treatment.

Recoil tests show a slight improvement of the compressive strength for cross-linked PPTA-co-5XTA fiber. Bending tests demonstrate a 100–200% increase in compressive strain to failure upon cross-linking for the PPXTA fiber.

The creep and creep rate of cross-linked PPXTA fibers are shown to be lower than those of un-cross-linked fibers. The cross-linked copolymer fibers also exhibit enhanced resistance to lateral compression.

Acknowledgment. This research was funded by the U. S. Army Advanced Concepts Technology Program through Grant DAAK60-92-K-0005. D.C.M. acknowledges support from the NSF in the form of a Young Investigator award. The authors thank Professor J. S. Moore for helpful discussion throughout this work. We also thank Dr. Joseph Manista and Dr. Robert Irwin of DuPont for spinning of the PPTA-co-5XTA and PPXTA fibers. Special thanks go to Professors John W. Halloran and J. C. Bilello for providing access to the fiber-

processing and mechanical-testing apparatus. Additional financial support came from DuPont and Hoechst-Celanese.

References and Notes

(1) Kwolek, S. L. U.S. Patent 3,671,542, 1972.
(2) Allen, S. R. *J. Mater. Sci.* **1987**, *22*, 853.
(3) Martin, D. C.; Thomas, E. L. *J. Mater. Sci.* **1991**, *26*, 5173.
(4) Dobb, M. G.; Johnson, D. J.; Saville, B. P. *Polymer* **1981**, *22*, 960.
(5) DeTeresa, S. J.; Porter, R. S.; Farris, R. J. *J. Mater. Sci.* **1985**, *22*, 1645.
(6) Wang, J. Z.; Dillard, D. A.; Ward, T. C. *J. Polym. Sci.* **1992**, *30*, 1391.
(7) Chuah, H. H.; Tsai, T. T.; Wei, K. H.; Wang, C. S.; Arnold, F. E. *Proc. ACS Div. Polym. Mater. Sci. Eng.* **1989**, *60*, 517.
(8) Lee, C. Y-C.; Santhosh, U.; Wang, C. S. *Proc. ACS Div. Polym. Mater. Sci. Eng.* **1990**, *62*, 81.
(9) Sweeny, W. J. *J. Polym. Sci., Polym. Chem. Ed.* **1992**, *30*, 1111.
(10) Kirchhoff, R. A.; Carriere, C. J.; Bruza, K. J.; Rondan, N. G.; Sammler, R. L. *J. Macromol. Sci., Chem.* **1991**, *A28*, 1079.
(11) Rickert, C.; Neuenschwander, P.; Suter, U. W. *Macromol. Chem. Phys.* **1994**, *195*, 511.
(12) Glomm, B.; Rickert, C.; Neuenschwander, P.; Suter, U. W. *Macromol. Chem. Phys.* **1994**, *195*, 525.
(13) Panar, M.; Avakian, P.; Blume, R. C.; Gardner, D. H.; Gierke, T. D.; Yang, H. H. *J. Polym. Sci.* **1983**, *21*, 1955.
(14) Dobb, M. G.; *Strong Fibres*; Watt, W., Perov, B. V., Eds.; Handbook of Composites; Elsevier Science Publishers B.V.; Amsterdam, 1985; Vol. 1, Chapter 17.
(15) Northolt, M. G. *Eur. Polym. J.* **1974**, *10*, 799.
(16) Haraguchi, K.; Kajiyama, T.; Takayanagi, M. *J. Appl. Polym. Sci.* **1979**, *23*, 915.
(17) Walker, K. A.; Markoski, L. J.; Deeter, G. A.; Spilman, G. E.; Martin, D. C.; Moore, J. S. *Polymer* **1994**, *35*, 5012.
(18) Markoski, L. J.; Walker, K. A.; Deeter, G. A.; Spilman, G. E.; Martin, D. C.; Moore, J. S. *Chem. Mater.* **1993**, *5*, 248.
(19) Spilman, G. E.; Markoski, L. J.; Walker, K. A.; Deeter, G. A.; Martin, D. C.; Moore, J. S. *Polym. Prep. (Am. Chem. Soc., Div. Polym. Chem.)* **1993**, *68*, 139.
(20) Blades, H. U.S. Patent 3,767,756, 1973.
(21) Blades, H. U.S. Patent 3,869,430, 1975.
(22) Hindeleh, A. M.; Abdo, S. M. *Polymer* **1989**, *30*, 218.
(23) Allen, S. R.; Farris, R. J.; Thomas, E. L. *J. Mater. Sci.* **1985**, *20*, 2727.
(24) Pottick, L. A.; Farris, R. J. *Polym. Eng. Sci.* **1991**, *31*, 1441.
(25) Sinclair, D. *J. Appl. Phys.* **1950**, *21*, 380.
(26) DeTeresa, S. J.; Allen, S. R.; Farris, R. J.; Porter, R. S. *J. Mater. Sci.* **1984**, *19*, 57.
(27) Maier, W.; Saupe, A. *Z. Naturforsch.* **1959**, *149*, 882.
(28) Picken, S. J. *Macromolecules* **1989**, *22*, 1766.
(29) Hudson, S. D.; Thomas, E. L. *Phys. Rev. A* **1991**, *44*, 812.
(30) Warner, M.; Wang, X. J. *Macromolecules* **1991**, *24*, 4932.
(31) Jones, M-C. G.; Jiang, T.; Martin, D. C. *Macromolecules* **1994**, *27*, 6507.
(32) Alexander, L. E. *X-Ray Diffraction Methods in Polymer Science*; Wiley-Interscience; New York, 1969.
(33) Penning, J. P.; Pras, H. E.; Pennings, A. J. *Colloid Polym. Sci.* **1994**, *272* (6), 664.
(34) Mielewski, D. F.; Martin, D. C.; Bauer, D. R. *Proc. ACS Div. Polym. Mater. Sci. Eng.* **1994**, *71*, 160.
(35) Marks, M. J.; Erskine, J. S.; McCrery, D. A. *Macromolecules* **1994**, *27*, 4114.
(36) Feldman, L.; Zihlif, A. M.; Farris, R. J.; Thomas, E. L. *J. Mater. Sci.* **1987**, *22*, 1199.
(37) Ericksen, R. H. *Polymer* **1985**, *26*, 733.
(38) Schuppert, A. A. *Makromol. Chem., Theory Simul.* **1993**, *2*, 643.
(39) Spilman, G. E.; Jiang, T.; Moore, J. S.; Martin, D. C. *Polym. Prepr. (Am. Chem. Soc., Div. Polym. Chem.)* **1994**, *35* (2), 667.
(40) Lee, C. Y.-C.; Santhosh, U. *Polym. Eng. Sci.* **1993**, *33*, 907.
(41) Sawyer, L. C.; Chen, R. T.; Jamieson, M. G.; Musselman, I. H.; Russell, P. E. *J. Mater. Sci.* **1993**, *28*, 225.
(42) Saw, C. K.; Collins, G. L. *Bull. Am. Phys. Soc.* **1993**, *38* (1), 420.

MA946088G